J|A|C|S
ARTICLES
Published on Web 06/18/2002

Metal Ion-Catalyzed Nucleic Acid Alkylation and Fragmentation

Kenneth A. Browne*

Contribution from Gen-Probe Incorporated, 10210 Genetic Center Drive, San Diego, California 92121

Received December 12, 2001

Abstract: Nucleic acid microarrays are a growing technology in which high densities of known sequences are attached to a substrate in known locations (addressed). Hybridization of complementary sequences leads to a detectable signal such as an electrical impulse or fluorescence. This combination of sequence addressing, hybridization, and detection increases the efficiency of a variety of genomic disciplines including those that profile genetic expression, search for single nucleotide polymorphisms (SNPs), or diagnose infectious diseases by sequencing portions of microbial or viral genomes. Incorporation of reporter molecules into nucleic acids is essential for the sensitive detection of minute amounts of nucleic acids on most types of microarrays. Furthermore, polynucleic acid size reduction increases hybridization because of increased diffusion rates and decreased competing secondary structure of the target nucleic acids. Typically, these reactions would be performed as two separate processes. An improvement to past techniques, termed labeling-during-cleavage (LDC), is presented in which DNA or RNA is alkylated with fluorescent tags and fragmented in the same reaction mixture. In model studies with 26 nucleotide-long RNA and DNA oligomers using ultraviolet/visible and fluorescence spectroscopies as well as high-pressure liquid chromatography and mass spectrometry, addition of both alkylating agents (5-(bromomethyl)fluorescein, 5- or 6-iodoacetamidofluorescein) and select metal ions (of 21 tested) to nucleic acids in aqueous solutions was critical for significant increases in both labeling and fragmentation, with ≥100-fold increases in alkylation possible relative to metal ion-free reactions. Lanthanide series metal ions, Pb^{2+}, and Zn^{2+} were the most reactive ions in terms of catalyzing alkylation and fragmentation. While oligonucleotides were particularly susceptible to fragmentation at sites containing phosphorothioate moieties, labeling and cleavage reactions occurred even without incorporation of phosphorothioate moieties into the RNA *and* DNA target molecules. In fact, LDC conditions were found in which RNA could be fragmented into its component monomers, allowing simultaneous sequencing from both the 5′- and the 3′-termini by mass spectrometry. The results can be explained by alkylation of the (thio)phosphodiester linkages to form less hydrolytically stable (thio)-phosphotriesters, which then decompose into 2′,3′-cyclic phosphate (or 2′-phosphate) and 5′-hydroxyl terminal products. Analysis of fragmentation and alkylation products of *Mycobacterium tuberculosis* (*Mtb*) ribosomal RNA (rRNA) transcripts by polyacrylamide gel electrophoresis was consistent with the model studies. Building upon these results, I found that products from *Mtb* rRNA amplification products were processed with fluorescent reporters and metal ions in a single reaction milieu for analysis on an Affymetrix GeneChip. Mild conditions were discovered which balanced the need for aggressive alkylation and the need for controlled fragmentation, advantageously yielding GeneChip results with greater than 98% of the nucleotides reported correctly relative to reference sequences, results sufficient for accurately identifying *Mtb* from other *Mycobacterium* species. Thus, LDC is a new, straightforward, and rapid aqueous chemistry that is based on metal ion-catalyzed alkylation and alkylation-catalyzed fragmentation of nucleic acids for analysis on microarrays or other hybridization assays and that, possibly, has utility in similar processing of other appropriately functionalized biomolecules.

Introduction

Nucleic acid hybridization techniques on membrane surfaces have been immensely important to the evolution of molecular biology,[1−4] yet these early manifestations were labor intensive and largely limited to relatively simple experimental designs. Through the rapid development in the synthesis of high-density patterns of nucleic acids on solid supports in the form of DNA microarrays (so-called DNA "chips"),[5−8] significant advances

* To whom correspondence should be addressed. E-mail: kenb@gen-probe.com. Phone: (858) 410-8853 (voice). Fax: (858) 410-8870.

(1) Gillespie, D.; Spiegelman, S. *J. Mol. Biol.* **1965**, *12*, 829−842.
(2) Southern, E. M. *J. Mol. Biol.* **1975**, *98*, 503−517.
(3) Kafatos, F. C.; Jones, C. W.; Efstratiadis, A. *Nucleic Acids Res.* **1979**, *7*, 1541−1552.
(4) Conner, B. J.; Reyes, A. A.; Morin, C.; Itakura, K.; Teplitz, R. L.; Wallace, R. B. *Proc. Natl. Acad. Sci. U.S.A.* **1983**, *80*, 278−282.
(5) Pease, A. C.; Solas, D.; Sullivan, E. J.; Cronin, M. T.; Holmes, C. P.; Fodor, S. P. A. *Proc. Natl. Acad. Sci. U.S.A.* **1994**, *91*, 5022−5026.
(6) Southern, E. M.; Case-Green, S. C.; Elder, J. K.; Johnson, M.; Mir, K. U.; Wang, L.; Williams, J. C. *Nucleic Acids Res.* **1994**, *22*, 1368−1373.
(7) Shalon, D.; Smith, S. J.; Brown, P. O. *Genome Res.* **1996**, *6*, 639−645.

10.1021/ja017746x CCC: $22.00

in the detailed analyses of nucleic acid sequences have become possible in recent years. At the extreme, this technology has led to massively parallel studies of genome expression levels with simultaneous observations of hundreds to thousands of genes spanning a continuum of activity levels.[9−15]

Hybridization alone does not deal with the issue of detection of complementary pairing events. Many of the original membrane-based methods relied upon hybridization of a radiolabeled probe and subsequent exposure to and development of X-ray film. The current DNA microarrays generally use fluorescent detection,[16−19] although other modes of reporting are certainly possible (radioactive,[6,20,21] chemiluminescent,[22] nanoparticle,[8] colorimetric,[23] electronic,[24] up-converting phosphor[25]). Fluorescent probes can be generated either pre- or postsynthetically, enzymatically, or chemically.[26−28] In the process of amplifying scarce nucleic acids for detection on microarrays, inclusion of fluorescently labeled primers or nucleotide triphosphates might alter amplified product, or amplicon, yield because of differences in enzyme affinity for the substrate (K_M) or rates of incorporation (k_{cat}). Furthermore, these effects might also differ among sequence contexts. To circumvent such problems, postsynthetic chemical labeling of amplicons is a favorable alternative.

It might also be useful to be able to label nucleic acids randomly or selectively. A variety of nucleophilic sites with differing reactivities are available on nucleic acids that can react with electrophilic moieties conjugated to various labels. While some alkylating agents are known to be selective for sulfur, sulfur is not typically present in polynucleic acids. Yet as a functional analogue of oxygen, sulfur can be incorporated into DNA or RNA during an amplification reaction, typically on a nucleobase or a phosphate linkage. Importantly, the nonbridging sulfur of a phosphorothioate is more nucleophilic than the nonbridging oxygens of a phosphodiester. Gish and Eckstein provided evidence that addition of an alkylating agent such as iodoethane to a ribonucleotide dimer linked by a phosphorothioate yields a triester intermediate.[29] Likewise, the McLaughlin group incorporated reporter molecules with γ-bromo-α,β-unsaturated carbonyl, haloacetamide, and aziridinyl sulfonamide functional groups onto phosphorothioate diesters.[30−32] Work from Czworkowski and co-workers indicated that incorporation of a phosphorothioate moiety into RNA transcripts facilitates alkylation of nucleic acids by iodoacetamido reagents.[33] Thus, use of thiophosphates in nucleic acids is a well-known technique to facilitate highly reactive and site-selective chemical labeling.

In processing labeled polynucleic acids for hybridization analysis, it often also becomes advantageous to degrade the polynucleic acids into smaller fragments to reduce secondary structure and steric hindrance as well as to increase hybridization kinetics.[34−36] Considerable attention has focused on hydrolysis of RNA catalyzed by metal ions[37−40] and by amines.[41−44] Phosphorothioate esters, including those incorporated into DNA or RNA, are typically more susceptible to chemical cleavage than are their analogous phosphate esters.[29,45−48] Thus, selective incorporation of phosphorothioates into the nucleic acid being studied could be doubly useful in that the phosphorothioates are reactive to both alkylation and fragmentation.

The current results build upon this chemical background with the design and implementation of a new methodology called labeling-during-cleavage (LDC[49]). This technique has the significant advantage of rapidly labeling single-stranded nucleic acids with a fluorescent tag and, in the same reaction mixture, fragmenting the nucleic acids into sizes appropriate for efficient detection on a microarray. In addition, LDC does not require preliminary modification of nucleic acids to yield functional groups such as aldehydes for attaching labels,[50,51] nor does it

(8) Taton, T. A.; Mirkin, C. A.; Letsinger, R. L. *Science* **2000**, *289*, 1757−1760.
(9) Schena, M.; Shalon, D.; Davis, R. W.; Brown, P. O. *Science* **1995**, *270*, 467−470.
(10) DeRisi, J.; Penland, L.; Brown, P. O.; Bittner, M. L.; Meltzer, P. S.; Ray, M.; Chen, Y.; Su, Y. A.; Trent, J. M. *Nat. Genet.* **1996**, *14*, 457−460.
(11) Wodicka, L.; Dong, H.; Mittmann, M.; Ho, M.-H.; Lockhart, D. J. *Nat. Biotechnol.* **1997**, *15*, 1359−1367.
(12) de Saizieu, A.; Certa, U.; Warrington, J.; Gray, C.; Keck, W.; Mous, J. *Nat. Biotechnol.* **1998**, *16*, 45−48.
(13) Duggan, D. J.; Bittner, M.; Chen, Y.; Meltzer, P.; Trent, J. M. *Nat. Genet.* **1999**, *21*, 10−14.
(14) Lockhart, D. J.; Winzeler, E. A. *Nature* **2000**, *405*, 827−836.
(15) Zarrinkar, P. P.; Mainquist, J. K.; Zamora, M.; Stern, D.; Welsh, J. B.; Sapinoso, L. M.; Hampton, G. M.; Lockhart, D. J. *Genome Res.* **2001**, *11*, 1256−1261.
(16) Cheng, J.; Sheldon, E. L.; Wu, L.; Uribe, A.; Gerrue, L. O.; Carrino, J.; Heller, M. J.; O'Connell, J. P. *Nat. Biotechnol.* **1998**, *16*, 541−546.
(17) Lipshutz, R. J.; Fodor, S. P. A.; Gingeras, T. R.; Lockhart, D. J. *Nat. Genet.* **1999**, *21*, 20−24.
(18) Singh-Gasson, S.; Green, R. D.; Yue, Y.; Nelson, C.; Blattner, F.; Sussman, M. R.; Cerrina, F. *Nat. Biotechnol.* **1999**, *17*, 974−978.
(19) Okamoto, T.; Suzuki, T.; Yamamoto, N. *Nat. Biotechnol.* **2000**, *18*, 438−441.
(20) Lamture, J. B.; Beattie, K. L.; Burke, B. E.; Eggers, M. D.; Ehrlich, D. J.; Fowler, R.; Hollis, M. A.; Kosicki, B. B.; Reich, R. K.; Smith, S. R.; Varma, R. S.; Hogan, M. E. *Nucleic Acids Res.* **1994**, *22*, 2121−2125.
(21) Schuchhardt, J.; Beule, D.; Malik, A.; Wolski, E.; Eickhoff, H.; Lehrach, H.; Herzel, H. *Nucleic Acids Res.* **2000**, *28*, E47.
(22) Rajeevan, M. S.; Dimulescu, I. M.; Unger, E. R.; Vernon, S. D. *J. Histochem. Cytochem.* **1999**, *47*, 337−342.
(23) Alexandre, I.; Hamels, S.; Dufour, S.; Collet, J.; Zammatteo, N.; De Longueville, F.; Gala, J.-L.; Remacle, J. *Anal. Biochem.* **2001**, *295*, 1−8.
(24) Umek, R. M.; Lin, S. W.; Vielmetter, J.; Terbrueggen, R. H.; Irvine, B.; Yu, C. J.; Kayyem, J. F.; Yowanto, H.; Blackburn, G. F.; Farkas, D. H.; Chen, Y. P. *J. Mol. Diagn.* **2001**, *3*, 74−84.
(25) van de Rijke, F.; Zijlmans, H.; Li, S.; Vail, T.; Raap, A. K.; Niedbala, R. S.; Tanke, H. J. *Nat. Biotechnol.* **2001**, *19*, 273−276.
(26) Wojczewski, C.; Stolze, K.; Engels, J. W. *Synth. Lett.* **1999**, *10*, 1667−1678.
(27) Neves, C.; Byk, G.; Escriou, V.; Bussone, F.; Scherman, D.; Wils, P. *Bioconjugate Chem.* **2000**, *11*, 51−55.
(28) Trévisiol, E.; Defrancq, E.; Lhomme, J.; Laayoun, A.; Cros, P. *Eur. J. Org. Chem.* **2000**, 211−217.
(29) Gish, G.; Eckstein, F. *Science* **1988**, *240*, 1520−1522.
(30) Hodges, R. R.; Conway, N. E.; McLaughlin, L. W. *Biochemistry* **1989**, *28*, 261−267.
(31) Fidanza, J. A.; McLaughlin, L. W. *J. Am. Chem. Soc.* **1989**, *111*, 9117−9119.
(32) Fidanza, J. A.; Ozaki, H.; McLaughlin, L. W. *J. Am. Chem. Soc.* **1992**, *114*, 5509−5517.
(33) Czworkowski, J.; Odom, O. W.; Hardesty, B. *Biochemistry* **1991**, *30*, 4821−4830.
(34) Hacia, J. G.; Brody, L. C.; Chee, M. S.; Fodor, S. P. A.; Collins, F. S. *Nat. Genet.* **1996**, *14*, 441−447.
(35) Southern, E.; Mir, K.; Shchepinov, M. *Nat. Genet*. **1999**, *21*, 5−9.
(36) Chan, V.; Graves, D. J.; McKenzie, S. E. *Biophys. J.* **1995**, *69*, 2243−2255.
(37) Kuimelis, R. G.; McLaughlin, L. W. *Biochemistry* **1996**, *35*, 5308−5317.
(38) Wrzesinski, J.; Michalowski, D.; Ciesiolka, J.; Krzyzosiak, W. J. *FEBS Lett.* **1995**, *374*, 62−68.
(39) Tsuruoka, H.; Shohda, K.-i.; Wada, T.; Sekine, M. *J. Org. Chem.* **1997**, *62*, 2813−2822.
(40) Zagórowska, I.; Kuusela, S.; Lönnberg, H. *Nucleic Acids Res.* **1998**, *26*, 3392−3396.
(41) Podyminogin, M. A.; Vlassov, V. V.; Giegé, R. *Nucleic Acids Res.* **1993**, *21*, 5950−5956.
(42) Kuimelis, R. G.; McLaughlin, L. W. *J. Am. Chem. Soc.* **1995**, *117*, 11019−11020.
(43) Vlassov, V. V.; Zuber, G.; Felden, B.; Behr, J.-P.; Giegé, R. *Nucleic Acids Res.* **1995**, *23*, 3161−3167.
(44) Bibillo, A.; Figlerowicz, M.; Kierzek, R. *Nucleic Acids Res.* **1999**, *27*, 3931−3937.
(45) Breslow, R.; Katz, I. *J. Am. Chem. Soc.* **1968**, *90*, 7376−7377.
(46) Kuimelis, R. G.; McLaughlin, L. W. *Nucleic Acids Res.* **1995**, *23*, 4753−4760.
(47) Catrina, I. E.; Hengge, A. C. *J. Am. Chem. Soc.* **1999**, *121*, 2156−2163.
(48) Mag, M.; Lüking, S.; Engels, J. W. *Nucleic Acids Res.* **1991**, *19*, 1437−1441.
(49) Monnot, V.; Tora, C.; Lopez, S.; Menou, L.; Laayoun, A. *Nucleosides Nucleotides* **2001**, *20*, 1177−1179.
(50) Wu, T.-P.; Ruan, K.-C.; Liu, W.-Y. *Nucleic Acids Res.* **1996**, *24*, 3472−3473.

Table 1. *Escherichia coli* Complementary 16S (c*Eco*A) rRNA Oligonucleotide Sequences and Modifications

Name[a]	Sequence[b,c]	MW (g mol^{-1})
	1105 1100 1095 1090 1085	
c*Eco*A1082-1107 [DNA]	5′-GCT CGT TGC GGG ACT T-**p**-AA CCC AAC AT-**OH**-3′	7932
c*Eco*A1082-1107 ps1092 [DNA]	5′-GCT CGT TGC GGG ACT T-**s**-AA CCC AAC AT-**OH**-3′	7948
c*Eco*A1082-1107 ps1082 [DNA]	5′-GCT CGT TGC GGG ACT T-**p**-AA CCC AAC AT-**s**-3′	8027
c*Eco*A1082-1107 ps1092 [RNA]	5′-GCU CGU UGC GGG ACU U-**s**-AA CCC AAC AU-**OH**-3′	8280
c*Eco*A1082-1107 ps1082 [RNA]	5′-GCU CGU UGC GGG ACU U-**p**-AA CCC AAC AU-**s**-3′	8359
c*Eco*A1092-1107 [RNA]	5′-GCU CGU UGC GGG ACU U-**OH**-3′	5090
c*Eco*A1092-1107 ps1092 [RNA]	5′-GCU CGU UGC GGG ACU U-**s**-3′	5185
c*Eco*A1082-1091 [RNA]	5′-AA CCC AAC AU-**OH**-3′	3111

[a] Numbered in the 5′ → 3′ orientation of the (+) sense rRNA sequence. [b] GenBank AE005174. [c] "**-p-**" and "**-s-**" indicate phosphate or thiophosphate moieties, respectively, and **-OH** denotes a terminal hydroxyl; all 5′-ends terminate in a hydroxyl.

require nucleic acid purification from complex mixtures such as enzymatic reactions. Small synthetic RNA *and* DNA oligomers, with or without phosphorothioate linkages, were initially used as model substrates, with a variety of buffers, metal ions, and fluorescent alkylating agents examined for efficacy in LDC. This work culminated in RNA amplicon product analyses of these LDC reactions as well as successful applications on the Affymetrix GeneChip.

Materials and Methods

Model Alkylation Reactions. Model alkylation reactions were performed as follows, with minor variations indicated in the Results and the figure legends: (1) total volume = 100 μL; (2) 9.3 μM polyacrylamide gel-purified oligonucleotide (Table 1; all oligonucleotides were synthesized in-house using phosporamidite chemistry on Expedite 8909 Systems (ABI, Foster City, CA)); (3) 50 mM buffer (e.g., MOPS pH 7.2, HEPES pH 7.6, imidazole pH 7.6, or Tris pH 8.1); (4) 0, 1−5 mM metal ion chlorides (e.g., Be^{2+}, Mg^{2+}, Cr^{3+}, Mn^{2+}, Co^{2+}, Ni^{2+}, Cu^{2+}, Zn^{2+}, Rb^{+}, Cd^{2+}, In^{3+}, Sn^{2+}, Cs^{+}, Ba^{2+}, Ce^{3+}, Eu^{3+}, Tb^{3+}, Tm^{3+}, Yb^{3+}, Lu^{3+}, or Pb^{2+}); (5) 0, 0.25−1.25 mM fluorescent alkylating agent (e.g., 5-(bromomethyl)fluorescein (5-BMF), 5- or 6-iodoacetamidofluorescein (5-IAF or 6-IAF), or fluorescein-5-maleimide (5-MaF); Chart 1) in 5% dimethyl formamide (DMF). Buffers, salts, and solvents were purchased from Sigma-Aldrich (St. Louis, MO), and alkylating agents were from Molecular Probes (Eugene, OR). Reagents were added in the order indicated, mixed by vortexing, and incubated at 60 °C. Except for time courses, the reactions were generally allowed to proceed for 30 min to balance completion of the different alkylation reactions with the higher throughput of shorter reaction times. The reactions were stopped by addition and mixing of 5 mM (final) EDTA. Unless stated otherwise, all reagents were dissolved/diluted in MilliQ 18 MΩ deionized H_2O (Millipore, Bedford, MA).

Chart 1. Electrophilic Fluorescein Derivatives

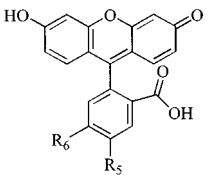

R_5 = -CH_2Br, R_6 = -H; 5-BMF

R_5 = -NHC(O)CH_2I, R_6 = -H; 5-IAF

R_5 = -H, R_6 = -NHC(O)CH_2I; 6-IAF

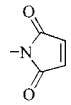

R_5 = , R_6 = -H; 5-MaF

After the alkylation reactions, the nucleic acids were purified by liquid−liquid extraction. Sodium acetate pH 5.0 (250 mM final) and 150 μL of H_2O-saturated *n*-butanol were added to the alkylation reactions and mixed by vortexing. After phase separation, the aqueous layer was re-extracted with 150 μL of H_2O-saturated *n*-butanol, and the nucleic acids from the aqueous phase were precipitated following addition of a 4-fold excess of cold ethanol (15 min on dry ice, centrifuged 19 000*g* for 15 min). The pellet was washed once with

(51) Proudnikov, D.; Mirzabekov, A. *Nucleic Acids Res.* **1996**, *24*, 4535−4542.

cold 70% ethanol, dried, and resuspended in 500 μL of 100 mM sodium carbonate pH 9.5.

Incorporation Efficiency. Incorporation efficiency was determined from UV/visible absorbance spectroscopy by (A) subtracting $0.214 \times A_{494}$ from A_{260} to correct oligonucleotide absorbance for the contribution at 260 nm because of overlap with fluorescein UV absorbance, (B) converting absorbance to concentration on the basis of the Beer−Lambert Law and the extinction coefficients $\epsilon_{494} = 0.080\ \mu M^{-1}\ cm^{-1}$ for fluorescein and $\epsilon_{260} = 0.214\ \mu M^{-1}\ cm^{-1}$ for 26 nt long oligonucleotides, and (C) calculating the fraction incorporated from eq 1:

$$\% \text{ incorporation} = \frac{[\text{fluorescein}]}{[\text{oligomer}]} \times 100 \qquad (1)$$

Recovery of the oligonucleotides was generally >90% except when Pb^{2+} was used (<33%). UV absorbance data for Ce^{3+} should be viewed cautiously because of the large UV absorbance of Ce^{3+} present after purification.

For a subset of conditions, absorbance quantification of alkylation was compared to fluorescent output. A total of 50 pmol of c*Eco*A1082-1107-3′-biotin [DNA] (i.e., the complementary sequence to c*Eco*A1082-1107 attached to a 3′-terminal biotin moiety) in 150 μL of 5× SSPEt (750 mM NaCl, 50 mM sodium phosphate pH 7.4, 5 mM EDTA, 0.05% Triton X-100) was allowed to bind to Streptavidin-coated surfaces in white Labsystems 96-well plates (Franklin, MA) for 30 min at room temperature. Wells were washed 3× with 150 μL of 5× SSPEt, and then 75 μL of 5× SSPEt was added to each well followed by 75 μL of each oligonucleotide alkylation condition (vide supra) in sodium carbonate buffer (or sodium carbonate without oligonucleotides for buffer background). The oligonucleotides were hybridized by incubating the solutions in the plate for 30 min at 50 °C, washing 3× with 150 μL of 5× SSPEt, and filling the wells with 150 μL of 5× SSPEt. Fluorescence from these solutions was read on a SPEX 1680 0.22 m Double Spectrometer with a MicroMax microplate adapter (Edison, NJ; Ex 495 nm, Em 525 nm; slits at 5 and 8 nm, respectively; 1 s read time).

High-Pressure Liquid Chromatography and Mass Spectrometry. Alkylation of model oligonucleotides was further characterized by high-pressure liquid chromatography (HPLC) and by mass spectrometry (MS). Approximately 1 nmol of selected oligonucleotides subjected to alkylation procedures (vide supra) was separated by reversed-phase (RP) HPLC (Beckman System Gold (Fullerton, CA); Phenomenex (Torrance, CA) 300 × 3.9 mm, 10 μm C18 column; linear gradient of 5−30% acetonitrile with H_2O containing 0.1 M triethylammonium acetate at 1 mL min^{-1} over 50 min), and the reaction products were detected by absorbance at 260 nm. Matrix-assisted laser desorption/ionization time-of-flight (MALDI-TOF) MS was performed on a PerSeptive Biosystems Voyager DE spectrometer (Framingham, MA; positive ion detection (m+1/z); accelerating voltage = 25 000 V; nitrogen laser (337 nm) intensity = 2100−2280 (ca. 116−126 μJ)). Following the alkylation reactions, 70 pmol of the oligonucleotides was incubated with a cation-exchange resin in 3 mM ammonium citrate (pH 9.4) and 220 mM 3-hydroxypicolinic acid; 14 pmol of the desalted oligonucleotides was air-dried on the sample plate for analysis. Masses were calibrated on c*Eco*A1092-1107 [RNA] as an external standard (Table 1). Small variations in TOF (∝ mass) were because of subtle differences in the position of the sample plate; hence, it is best to consider much of the data in terms of differences in masses.

The Polymerase Chain Reaction (PCR). The polymerase chain reaction was run essentially as recommended for *Pfu* DNA polymerase (Stratagene; La Jolla, CA). Briefly, 200 μM of each dNTP, 0.5 μM of each primer (5′-GAACGGAAAGGTCTCTTCGGAGATACTC-3′ (*Mtb*27-54(+)) and 5′-**GAAATTAATACGACTCACTATAGGGAG-ACCACA**TTGTGCAATATTCCCCACTGC-3′ (T7-*Mtb*313-333(−)); bold region indicates a noncomplementary T7 RNAP promoter sequence), 10 ng of a plasmid construct containing *Mtb* 16S ribosomal sequence (GenBank X52917),[52] and 5 U of *Pfu* DNA polymerase were mixed. After 30 cycles of 96 °C/1 min, 45 °C/1 min, and 72 °C/2 min (PE GeneAmp PCR System 9600; Foster City, CA), the synthesized DNA was purified with a QIAquick PCR kit (QIAGEN; Valencia, CA) and quantified by UV spectroscopy (50 $\mu g/OD_{260}$).

Transcription. Transcription products were synthesized using AMBION MEGAscript T7 RNA polymerase kit (Austin, TX) and recommended conditions. Briefly, 7.5 mM of each rNTP plus 20 μCi of [α-^{32}P]UTP (AP Biotech; Piscataway, NJ), 0.54 μg of *Mtb* 16S PCR product, and 2 μL of T7 RNAP enzyme mixture were combined in order and mixed. After incubating at 37 °C for 3 h, the DNA was degraded with 2 U of DNase I at 37 °C for 15 min. Full-length (313 nt) transcripts were separated from premature sequences on a 6% acrylamide/7 M urea gel and extracted from the gel matrix by incubating in 50 mM ammonium acetate/1 mM EDTA at 60 °C for 2 h. The RNA was purified with a RNeasy Mini RNA kit (QIAGEN), quantified by UV spectroscopy (40 $\mu g/OD_{260}$), and the radiolabel incorporation was measured by scintillation counting.

Transcription-Mediated Amplification (TMA).[53] Transcription-mediated amplification was performed in 12 × 75 mm polypropylene tubes with a total aqueous volume of 100 μL. Primers (same as for PCR) were added to amplification reagent (final concentrations; 75 nM each primer, 40 mM Tris, 17.5 mM KCl, 20 mM $MgCl_2$, 1 mM each dNTP, 4 mM each rNTP, 5% poly(vinylpyrrolidone) (w/v, average MW $\approx$ 40 000 g mol^{-1}), pH = 7.5) and covered with 200 μL of silicone oil to prevent evaporation and sample cross-contamination. RNA transcripts or ribosomal RNA were diluted into H_2O, and either 1000 copies or H_2O were added to the primers (positive and negative amplifications, respectively), the tubes sealed, the solutions mixed by shaking, and primers and target hybridized in a 60 °C circulating water bath. After 10 min, the reactions were transferred to a 42 °C water bath and equilibrated for 10 min. A solution of enzyme reagent (final concentrations; 35 mM Tris, 2 mM HEPES, 17.5 mM KCl, 0.26 mM EDTA, 12.5 mM *N*-acetyl-L-cysteine, 2.52% Triton X-102, 0.76% (+)-D-trehalose, 0.01 mM zinc acetate, 5% glycerol, pH = 7.9; 2000 U of Moloney Murine Leukemia Virus Reverse Transcriptase (MMLV RT) and 2000 U of T7 RNA polymerase (RNAP) where 1 U = 5.75 fmol of cDNA synthesized in 15 min at 37 °C and 5 fmol transcript synthesized in 20 min at 37 °C for RT and RNAP, respectively) was then added to the nucleic acid primer-template hybrids and gently mixed. Incubation continued for 60 min at 42 °C.

Labeling and Fragmentation. Labeling and fragmentation of amplified RNA (amplicons) for polyacrylamide gel electrophoretic analysis were conducted in the post-TMA reaction milieu. In 100 μL, 5 μL of a *Mtb* 16S TMA reaction was mixed with either H_2O or 10^{13} copies of ^{32}P-labeled *Mtb* rRNA from the transcription reaction, 6−50 mM imidazole (pH 6.0−7.6), MOPS pH 7.6 or Tris pH 7.6, and up to 60 mM Mn^{2+}, 10 mM Zn^{2+}, or 5 mM Ce^{3+}. Either 0.01, 0.1, or 1.0 mM 5-BMF was included in the reactions as the fluorescent alkylating agent. After vortexing, the samples were incubated at 60 °C for 30 min, and then stored at −20 °C until analyzed. PAGE separation consisted of loading 15 μL of a 1:1 mixture of the alkylation reaction and 2× formamide loading buffer on a preheated 33 cm × 30 cm × 0.4 mm 6% acrylamide gel (19:1) containing 7 M urea in 1× TBE (100 mM Tris base, 88 mM boric acid, 2 mM EDTA, pH $\approx$ 8) after denaturing at 95 °C for 5 min. The gel was run at 40 W constant for 70 min prior to imaging fluorescein fluorescence on a Molecular Dynamics Storm 860 (Sunnyvale, CA) at 200 μm resolution. A phosphor screen was then exposed to the gel overnight for subsequent imaging of the ^{32}P-labeled fragments on the Molecular Dynamics Storm. Using ImageQuant v. 5.1, the results were quantified from either a

(52) Rogall, T.; Wolters, J.; Flohr, T.; Bottger, E. C. *Int. J. Syst. Bacteriol.* **1990**, *40*, 323−330.
(53) Brentano, S. T.; McDonough, S. H. In *Nonradioactive Analysis of Biomolecules*; Kessler, C., Ed.; Springer-Verlag: New York, 2000; pp 374−380.

33.5 mm^2 area around each full-length ^{32}P-labeled transcript or a 290 mm^2 rectangular area around the ~26−106 nt (between the xylene cyanole and the bromphenol blue bands) ^{32}P-labeled and fluorescein-labeled fragments.

GeneChip Analysis. RNA products from TMA reactions were conjugated with a fluorescein-alkylating agent and fragmented using optimizations of protocols described above. Briefly, 50 μL of a TMA reaction was mixed to a final concentration of 30 mM imidazole, 30 mM $MnCl_2$, and 1 mM 5-BMF in 250 μL total, and this solution was incubated at 60 °C for 30 min (with variations indicated in the Results). One hundred microliters of the processed reactions was diluted with 700 μL of hybridization buffer (900 mM NaCl, 60 mM HEPES pH 7.0, 3 M betaine, 16 mM EDTA, 1% dodecyltrimethylammonium bromide (DTAB), 250 μg mL^{-1} salmon sperm DNA, 6.25 nM control oligonucleotide (5′-fluorescein-CTGAACGGTAGCATCTTGAC-3′), 0.1% Foam-Ban MS-575). This solution was incubated and mixed in an Affymetrix BMX-MYCO GeneChip[54] on an Affymetrix GeneChip Fluidics Station (Santa Clara, CA) at 45 °C for 30 min. (This GeneChip design is composed of a series of overlapping 17 nt DNA probe sets (tiles) for determining the sequence of a 185 nt region of *Mtb* 16S rRNA. Each tile includes four probes differing by a single interior nt (interrogation position); one probe is the exact complement to the *Mtb* reference sequence, while the remaining three probes are possible single base mismatches.) The solution containing unhybridized RNA and excess fluorophore was drained, and the GeneChip was cleaned of nonspecifically bound compounds with ≥5 repeated exchanges of wash buffer (600 mM NaCl, 60 mM HEPES pH 7.4, 3 mM EDTA, 0.2% DTAB) at 30 °C. The GeneChip was then filled with read buffer (450 mM NaCl, 60 mM HEPES pH 7.4), and fluorescent signals emitted from bound target were detected at 6 μm resolution with a Hewlett-Packard GeneArray scanner (Palo Alto, CA). The GeneChip software (Affymetrix) generated reports containing probe array median fluorescence intensities and fraction of nt correctly identified (percent correct of 185 nt).

Results

Model System Design. In support of labeling RNA amplicons for subsequent fluorescent detection on an Affymetrix GeneChip, a 26 nucleotide (nt) region complementary to *E. coli* O157:H7 16S rRNA (Table 1)[55] was chosen as a moderately structured, single-stranded model nucleic acid system for detailed alkylation analysis. Various metal ions were included in the nucleic acid/alkylating agent mixtures in an attempt to drive both alkylation and metal ion-catalyzed fragmentation of nucleic acids in the same solution, thereby simplifying and reducing the time required for nucleic acid processing. Preliminary experiments suggesting that metal ions catalyze alkylation with alkyl halide- and haloacetamide-activated fluorescein derivatives were supported by the result that inclusion of as little as a 2-fold molar excess of EDTA over metal ion concentration maintains labeling at background levels. On the other hand, limited studies with maleimide-fluorescein conjugates indicated that alkylation by maleimide was not significantly catalyzed by Mn^{2+} or Zn^{2+}. In the subsequent paragraphs, time, buffer, alkylating agent and metal ion species, and thiophosphate position dependencies on alkylation and fragmentation of model oligonucleotides were evaluated by UV/visible and fluorescence spectroscopy, HPLC, and mass spectrometry. The conclusions from these experiments were used to initiate labeling-during-cleavage (LDC) optimizations of polynucleic acids prior to product analysis by gel electrophoresis and on DNA microarrays.

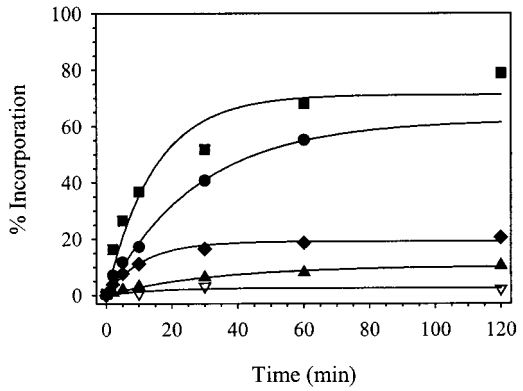

Figure 1. Time courses of 6-IAF incorporation onto c*Eco*A1082-1107 ps1092 [DNA]; 50 mM imidazole pH 7.6, 0.25 mM 6-IAF, ±5 mM metal ions, 60 °C. Curves through data points are theoretical fits to a first-order expression for the appearance of alkylated product, $y = A(1 - e^{(-kt)})$. H_2O (▽); Mn^{2+} (▲); Tb^{3+} (◆); Ce^{3+} (●); Zn^{2+} (■).

Time Dependence of Labeling. To determine the minimum reaction time until maximum alkylation extent, the 26 nt long DNA oligomer with an internal thiophosphate, c*Eco*A1082-1107 ps1092 [DNA], was allowed to react with either 5-(bromomethyl)fluorescein (5-BMF) or 6-iodoacetamidofluorescein (6-IAF) for various times. The products were worked up by organic extraction and precipitation, and the fraction alkylated was quantified using absorbance measurements and eq 1.

From Figure 1, it is clear that up to 60 min were required for maximal alkylation of DNA with 6-IAF at 60 °C. In addition, this preliminary work demonstrated that inclusion of some metal ions in the reaction solution, especially Zn^{2+} and Ce^{3+}, significantly increased the reaction yield but not the pseudo first-order rate constant ($k_{obsd} \approx 0.03-0.09$ min^{-1} in each 6-IAF case). The lack of a simple mathematical function relating alkylation yields and rate constants may be because of metal ion catalysis of reactions between the iodoacetamido moiety and water having a different metal ion specificity than that of the metal ion-catalyzed reactions between the iodoacetamido moiety and the nucleic acid functional groups (vide infra).

While alkylation was largely complete by the times indicated above, it was not clear which reagent was limiting. c*Eco*A1082-1107 ps1092 [DNA] was subjected to the same conditions as above for 30 min, and then a 10 μL aliquot of either H_2O (control), oligonucleotide, fluorescein-tagged alkylating agent, or metal ion was added for 30 min longer. The H_2O, oligonucleotide, or metal ion aliquots did not increase fluorescent incorporation, but addition of 6-IAF significantly increased alkylation (especially in the cases of Zn^{2+} and Ce^{3+}, 30 and 40%, respectively; data not shown). Furthermore, there was a large increase in alkylation when 5 mM Zn^{2+} was added to a metal ion-free reaction (no added metal ion for the first 30 min). Combined with the preceding statement, this suggests that a competing hydrolysis reaction of the alkylating agent is also metal ion-dependent.

Dependence on Buffer and Metal Ion Type. Once it was determined that metal ions catalyzed alkylation of nucleic acids

(54) Troesch, A.; Nguyen, H.; Miyada, C. G.; Desvarenne, S.; Gingeras, T. R.; Kaplan, P. M.; Cros, P.; Mabilat, C. *J. Clin. Microbiol.* **1999**, *37*, 49−55.
(55) Perna, N. T.; Plunkett, G., III; Burland, V.; Mau, B.; Glasner, J. D.; Rose, D. J.; Mayhew, G. F.; Evans, P. S.; Gregor, J.; Kirkpatrick, H. A.; Pósfai, G.; Hackett, J.; Klink, S.; Boutin, A.; Shao, Y.; Miller, L.; Grotbeck, E. J.; Davis, N. W.; Lim, A.; Dimalanta, E. T.; Potamousis, K. D.; Apodaca, J.; Anantharaman, T. S.; Lin, J.; Yen, G.; Schwartz, D. C.; Welch, R. A.; Blattner, F. R. *Nature* **2001**, *409*, 529−533.

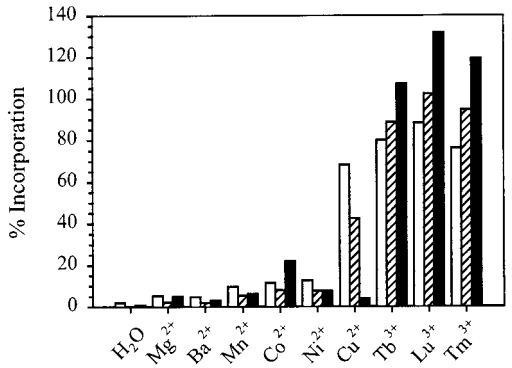

Figure 2. Plot of percent fluorescein incorporation versus metal ions and buffers for c*Eco*A 1082-1107 ps1092 [DNA]; 50 mM buffer, 1.25 mM 5-BMF, ±1 mM metal ions, 60 °C, 30 min. MOPS pH 7.2 (white); HEPES pH 7.6 (hatched); Tris pH 8.1 (black).

and that the time dependence of these reactions was approximately uniform, different metal ions were screened against each other in different buffers to optimize labeling with fluorescent moieties. Alkylation of c*Eco*A1082-1107 ps1092 [DNA] with 5-BMF was tested in conjunction with three amine buffers (MOPS, HEPES, Tris; preliminary experiments indicated that alkylation was much less efficient in phosphate and carbonate buffers; data not shown) and nine metal ions. The extent of DNA alkylation with 5-BMF generally varied little with the different buffers (pH 7.2−8.1), suggesting that there was little amine buffer or pH dependence in the range examined (Figure 2). (The Cu^{2+} in Tris buffer was an exception, with less than 5% incorporation as compared to 45 and 70% in HEPES and MOPS buffers, respectively. This could be a precipitation phenomenon because the solubility of Cu^{2+} decreases rapidly with increasing pH, because of selective complexation between Cu^{2+} and Tris, or because of a hyperreactive Tris-Cu^{2+} combination that hydrolyzes DNA into fragments that do not precipitate efficiently.) Specific metal ions, on the other hand, were critical for efficient DNA alkylation; in water alone, there was almost no alkylation by 5-BMF. Tb^{3+}, Tm^{3+}, Lu^{3+}, and Cu^{2+} catalyzed fluorescein incorporation to at least 40% and often to over 80%; values near and *exceeding* 100%, more than 100-fold increases over the uncatalyzed reactions, were also seen. This suggests that multiple alkylation events are possible on a nucleic acid strand (vide infra).

Dependence on Metal Ions and Thiophosphate Position. Past work suggests that thiophosphate substitutions in nucleic acids are more easily alkylated and chemically cleaved than phosphate linkages in DNA or RNA.[29−33,45−48] As an extension of the literature and the above metal ion-catalyzed alkylation results with standard nucleic acids, the effect of using oligonucleotides with internal or 3′-terminal thiophosphate moieties (c*Eco*A1082-1107 ps1092 [DNA] and c*Eco*A1082-1107 ps1082 [DNA], respectively) with 5-BMF and 6-IAF as alkylating agents was compared in the absence and presence of metal ions in Tris pH 8.1. This led to a "map" of the fluorescein labeling of internal or 3′-terminal thiophosphate DNA for the two alkylating agents and 15 metal ions (Table 2). While there was essentially no amine buffer dependence on alkylation (vide supra), metal ion species and position of the thiophosphate were very influential. The basal activities of 5-BMF and 6-IAF differed by about 3-fold (H_2O control), while the reactivities of internal and terminal thiophosphates to alkylating agents in the absence of metal ions differed by about 20-fold. 5-BMF was overall more sensitive to the presence of metal ions than was 6-IAF.

Table 2. Percent Fluorescein Incorporation with Different Alkylating Agents, Metal Ions, and Oligonucleotides[a,b]

	c*Eco*A1082-1107 ps1092 [DNA]		c*Eco*A1082-1107 ps1082 [DNA]	
	5-BMF	6-IAF	5-BMF	6-IAF
H_2O (control)	0.933	3.10	20.8	58.6
Yb^{3+}	78.7	48.4	98.6	60.9
Ce^{3+}	62.9	46.7	69.4	56.5
Tb^{3+}	51.8	45.4	66.9	64.2
In^{3+}	44.8	32.7	42.8	34.1
Pb^{2+}	43.6	54.5	59.8	69.0
Cr^{3+}	24.5[c]	29.8[c]	33.7[c]	62.3[c]
Zn^{2+}	21.1	20.5	13.6	36.0
Be^{2+}	12.6	10.4	13.5	27.0
Cd^{2+}	4.38	4.70	5.72	22.3
Co^{2+}	3.94	5.52	17.2	61.2
Sn^{2+}	3.59	4.13	23.1	50.2
Mn^{2+}	2.70	2.50	28.4	63.7
Ni^{2+}	1.70	2.22	19.5	67.0
Cs^{+}	1.17	1.12	22.0	58.7
Rb^{+}	1.04	1.09	20.4	57.8

[a] 50 mM Tris pH 8.1, 0.25 mM 5-BMF or 6-IAF, ±1 mM metal ion, 60 °C, 30 min. [b] Data sorted in descending order on the basis of alkylation of c*Eco*A1082-1107 ps1092 [DNA] by 5-BMF. [c] Data for Cr^{3+} should be viewed cautiously; see Figure 3.

The alkali metal ions (Rb^{+} and Cs^{+}) had no effect above that of H_2O alone for either of the oligonucleotides or alkylating agents; this is not surprising because these metal ions are from the same periodic group as Na^{+}, which was already present (from the buffer) at concentrations much greater than 1 mM. Addition of the Yb^{3+}, Ce^{3+}, and Tb^{3+} to DNA and 5-BMF resulted in much more fluorescein incorporation than was found with other metal ions; a 50−80-fold increase over the uncatalyzed reaction resulted when the lanthanides were incubated with 5-BMF. In addition to the lanthanides, In^{3+}, Pb^{2+}, Zn^{2+}, and Be^{2+} significantly stimulated alkylation of the oligonucleotide containing an internal thiophosphate with both 5-BMF and 6-IAF, while the remaining metal ions had little to no effect on alkylation. This metal ion pattern was largely paralleled by reactions with 5-BMF and the terminal thiophosphate DNA. Interestingly, inclusion of Zn^{2+}, Be^{2+}, and Cd^{2+} decreased the alkylation of terminal thiophosphate DNA with 5-BMF. Decreases in alkylation were even more pronounced for 6-IAF and the oligonucleotide containing a terminal thiophosphate; Zn^{2+}, Be^{2+}, Cd^{2+}, and In^{3+} reduced labeled product yield by ca. 50%. On the other hand, only two metal ions, Pb^{2+} and Ni^{2+}, increased alkylation when labeling the 3′-thiophosphate DNA with 6-IAF. Thus, while higher valent metal ions tend to catalyze alkylation of DNA, adjusting metal ions, alkylating agents, and the position of a thiophosphate substitution affords some alkylation selectivity.

Fluorescence Output as a Function of Labeling. For the LDC technique to be useful in the quantitative analysis of nucleic acids hybridized to microarrays (vide infra), the fluorescent output must be proportional to the number of fluorescent moieties incorporated into the oligonucleotides. This was done by comparing fluorescence yield to percent fluorescein incorporation of RNA containing internal or 3′-terminal thiophosphates after labeling with 5-IAF or 6-IAF in the absence or presence of metal ions. The above work demonstrated that certain metal ions, especially those in the +3 oxidation state,

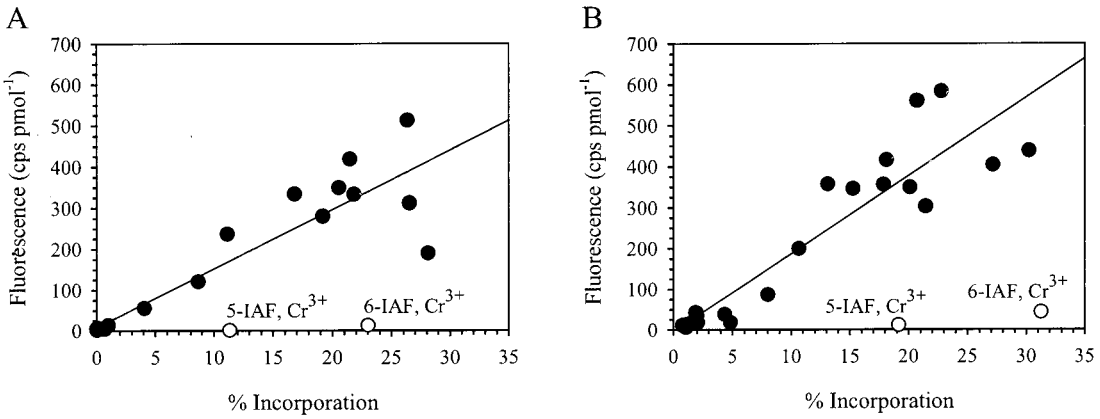

Figure 3. Relationship between fluorescence intensity and percent incorporation for the oligomers (A) c*Eco*A1082-1107 ps1092 [RNA] and (B) c*Eco*A1082-1107 ps1082 [RNA]; 50 mM buffer, 0.25 mM 5- or 6-IAF, ±1 mM metal ions, 60 °C, 30 min. For linear regressions, fluorescence = (A) 14.4 × % incorporation + 9.43 and (B) 19.0 × % incorporation − 2.75; $R^2 > 0.83$, $P < 0.001$ for each regression. Outliers (○) are from reactions with Cr^{3+} and were not used in the regressions.

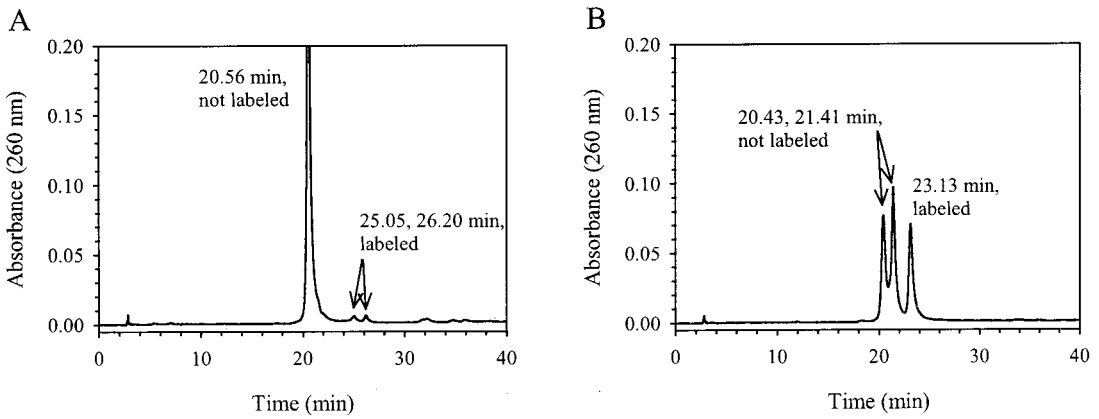

Figure 4. HPLC traces of incorporation of 5-BMF onto (A) c*Eco*A1082-1107 [DNA] and (B) c*Eco*A1082-1107 ps1082 [DNA]; 50 mM Tris pH 8.1, 0.25 mM 5-BMF, 1 mM Mn^{2+}, 60 °C, 30 min.

enhance alkylation of single-stranded DNA containing thiophosphates. As with DNA, labeling of RNA was metal ion and alkylating agent sensitive. Both 5-IAF and 6-IAF labeled thiophosphate RNA to similar extents, with 3′-thiophosphate RNA generally being labeled with slightly higher efficiency than RNA with a phosphorothioate. The presence of trivalent metal ions or Pb^{2+} greatly increased alkylation with 5-IAF and 6-IAF. Alkylation of thiophosphate-containing RNA oligomers did not appear to be as efficient as for thiophosphate-containing DNA, but the same metal ions which catalyzed alkylation of thiophosphate DNA improved labeling of thiophosphate RNA.

The fluorescein-labeled RNA oligomers yielded varying degrees of fluorescence, correlating linearly with the amount of fluorescein incorporation (Figure 3). Although phosphate and thiophosphate monoesters hydrolyze more rapidly than do their diesters, and thiophosphate monoesters hydrolyze more rapidly than do phosphate monoesters,[47] it was unlikely that significant hydrolysis of thiophosphate monoesters was occurring under the conditions employed because the conditions tested yielded similarly efficient labeling of RNA oligomers containing phosphorothioate and terminal thiophosphate moieties. Interestingly, the fluorescent yield on terminal thiophosphates was higher than that on phosphorothioates (compare slopes in Figure 3), possibly because of less fluorescence quenching on the terminus than on interior sites. The fluorescent response because of excess Cr^{3+} with both 5-IAF and 6-IAF and both thiophosphate-containing RNA oligomers was anomalously low relative to the percent incorporation. This could either be because of fluorescence quenching by Cr^{3+} or be because of Cr^{3+} absorbing at 494 nm, resulting in overcalculation of the amount of fluorescein incorporated. Supporting this second hypothesis, the absorbance of Cr^{3+} ($\epsilon_{494} \approx 0.26$ mM^{-1} cm^{-1}) was sufficient under the conditions of these experiments to influence the calculation of the relative fluorophore concentration.

Product Analysis by HPLC. Experiments such as those shown in Figure 2 indicate that greater than 100% incorporation of fluorescein into oligonucleotides is possible using certain combinations of buffers, alkylation agents, metal ions, and concentrations. Unfortunately, UV/visible spectroscopy alone does not differentiate between these products being a homogeneous or a heterogeneous population of labeled molecules. Results of HPLC separation and quantification of fluorescein-labeled and unlabeled peaks validated those values determined by UV/visible spectroscopy. Small, but measurable, amounts of fluorescein incorporation were seen on the oligomer c*Eco*A1082-1107 [DNA] following alkylation with 5-BMF and Mn^{2+} (Figure 4A). These products accounted for 1.6% (by area) of the total separated material, corresponding closely to the value based on absorbance in solution (1.9%). Similarly, quantification of the same labeling procedure for c*Eco*A1082-1107 ps1082 [DNA] in Figure 4B was quite similar by HPLC separation (27.9%) and by absorbance spectroscopy (28.4%). Unlike the

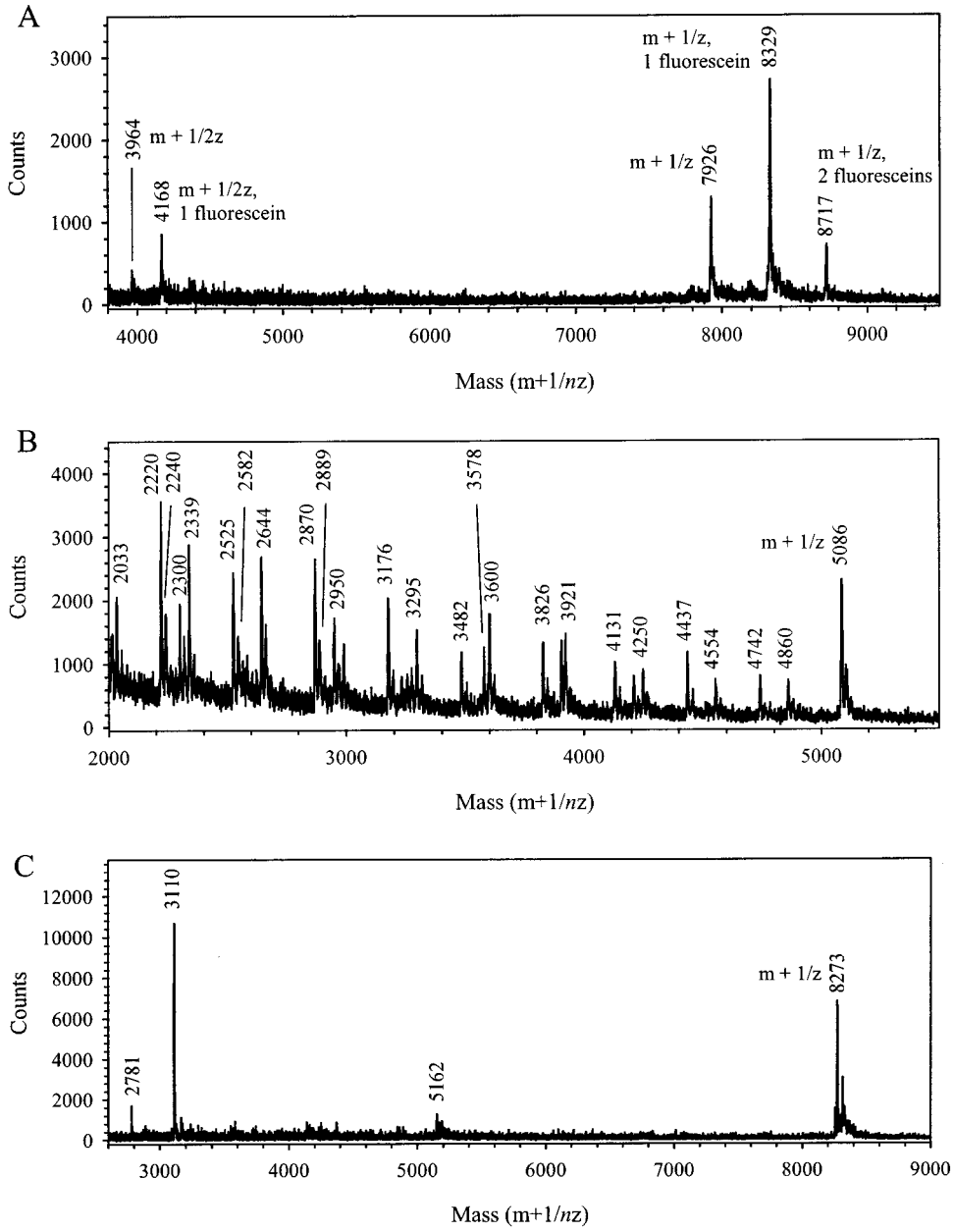

Figure 5. Examples of MALDI-TOF MS spectra for (A) c*Eco*A1082-1107 ps1092 [DNA], 0.25 mM 6-IAF, Zn^{2+}, (B) c*Eco*A1092-1107 [RNA], 0.25 mM 6-IAF, Tb^{3+}, and (C) c*Eco*A1082-1107 ps1092 [RNA], Zn^{2+}; 50 mM imidazole pH 7.6, 2.5 mM metal ions, 60 °C, 60 min. The masses of the peaks are shown vertically.

entirely phosphate DNA example, in which two, descrete labeled peaks were observed (accounting for labeling at two different sites either on separate oligonucleotides or on the same oligonucleotide; either condition could lead to different mobility on HPLC), the 3′-terminal thiophosphate DNA oligomer was highly susceptible to alkylation, likely at a single site.

Product Analysis by Mass Spectrometry. While HPLC analysis is quantitative, it was not useful in determining the mode of multiple labeling events, whether multiple alkylation events can occur on a single oligonucleotide or there are different preferential labeling sites on a single sequence. To differentiate these possibilities, alkylation was quantified by absorbance spectroscopy and compared with oligonucleotides separated and identified by MALDI-TOF MS. While the presence of a mass spectral peak is indicative of a particular species, one cannot necessarily conclude the absence of a chemical species by the absence of a calculated peak; some of the following results may fall within this caveat.

Representative examples of the MALDI-TOF MS data are shown in Figure 5. Full-length phosphorothioate-containing DNA with both one and two incorporated fluorescein moieties was seen following labeling with 6-IAF in the presence of Zn^{2+} (Figure 5A) and with 5-BMF/Zn^{2+} (Table 3). This combined with the HPLC data suggest that post-LDC oligonucleotides can be part of a heterogeneous population, likely composed of singly and doubly labeled species with discrete sites of alkylation. In a similar reaction involving 6-IAF/Tb^{3+} and RNA, a significant fragmentation pattern was seen (Figure 5B) that was not visible in the absence of Tb^{3+} (Table 3). In fact, the first nine nucleotides from the 5′-terminus were readily sequenced by mass difference; the mass at 4742 accounts for loss of 5′-Gp, at 4437 for −5′-GCp, at 4131 for −5′-GCUp, at 3826 for −5′-

Table 3. Products of Alkylating Agents and Metal Ions on (A) Fluorescein Incorporation and (B) Fragmentation of RNA and DNA Oligomers Determined by MALDI-TOF Mass Spectrometry[a,b]

A. Fluorescein Incorporation[c]

alkylating agent	metal ion	c*Eco*A1092-1107 ps1092 [RNA]	c*Eco*A1092-1107 [RNA]	c*Eco*A1082-1107 ps1092 [RNA]	c*Eco*A1082-1107 ps1092 [DNA]
5-BMF	Zn^{2+}	+ (34.0)	++ (48.4)	+ (40.6)	++ (119)
	Tb^{3+}	− (23.2)	ND (23.9)	− (15.3)	+ (31.1)
	H_2O	− (5.2)	− (0.5)	− (5.0)	− (0.7)
6-IAF	Zn^{2+}	− (21.0)	− (27.0)	+ (31.3)	++ (125)
	Tb^{3+}	− (8.2)	− (6.3)	ND (4.8)	− (16.0)
	H_2O	− (3.9)	− (0.6)	− (0.9)	− (1.6)

B. Fragmentation[d]

alkylating agent	metal ion	c*Eco*A1092-1107 ps1092 [RNA]	c*Eco*A1092-1107 [RNA]	c*Eco*A1082-1107 ps1092 [RNA]	c*Eco*A1082-1107 ps1092 [DNA]
5-BMF	Zn^{2+}	++	+++	++	−
	Tb^{3+}	++	ND	+++	++
	H_2O	−	−	+	−
6-IAF	Zn^{2+}	−	−	++	−
	Tb^{3+}	++	+++	ND	++
	H_2O	−	−	+	−

[a] Imidazole pH 7.6, 2.5 mM metal ion, 0.25 mM alkylating agent. [b] ND indicates not detected. [c] In (A), "−" indicates no fluorescein labeled oligonucleotides detected, "+" indicates monofluorescein labeled oligonucleotide detected, and "++" indicates mono- and difluorescein labeled oligonucleotide detected. Numbers in parentheses are absorbance spectroscopy-determined percent fluorescein incorporation values. [d] In (B), "−" indicates no fragmentation products detected, "+" indicates 2−5 fragmentation products/groups, "++" indicates 8−12 fragmentation products, and "+++" indicates >15 fragmentation products.

GCUCp, at 3482 for −5′-GCUCGp, at 3176 for −5′-GCUCGUp, at 2870 for −5′-GCUCGUUp, at 2525 for −5′-GCUCGUUGp, and at 2220 for −5′-GCUCGUUGCp. Likewise, the more subtle secondary fragmentation pattern demonstrated the loss of the 3′-nucleoside followed by sequential loss of eight nucleotides from the 3′-terminus; the mass at 4860 accounts for loss of 3′-U, at 4554 for −3′-UU, at 4250 for −3′-UUC, at 3921 for −3′-UUCA, at 3578 for −3′-UUCAG, at 2889 for −3′-UUCAGGG, at 2582 for −3′-UUCAGGGC, and at 2240 for −3′-UUCAGGGCG. Other conditions, including RNA plus 5-BMF/Zn^{2+} or 5-BMF/Tb^{3+}, also lead to mass differences that could allow sequencing (data not shown). Note that the phosphate moiety is associated with the 3′-terminus of the 5′-fragment and that none of the RNA peaks in this figure appear to be alkylated with a fluorescein group. In the absence of alkylating agent but presence of Zn^{2+}, c*Eco*A1082-1107 ps1092 [RNA] fragmented specifically into "c*Eco*A1092-1107 ps1092 [RNA]" and the remaining 10 3′-nt, c*Eco*A1082-1091 [RNA] (peaks corresponding to masses 5162 and 3110 g mol^{-1}, respectively; Figure 5C). Addition of alkylating agents to this oligonucleotide in the absence of metal ions resulted in the same fragments (data not shown).

These results, along with the remaining 5-BMF and 6-IAF, ±Zn^{2+} or Tb^{3+}, results, are qualitatively scored and summarized in Table 3 for MALDI-TOF MS and UV/visible spectroscopy. As shown above, both singly and doubly fluorescein-labeled oligonucleotides were generated from 5-BMF in the presence of Zn^{2+}, while only a singly alkylated DNA oligomer was detected in the presence of Tb^{3+}; no labeling was detected by mass spectrometry in the absence of metal ions (Table 3A). Mass spectrometry detected singly and doubly alkylated oligonucleotides only when labeling (by absorbance) was greater than ∼30 and 40%, respectively. Fluorescein incorporation was efficient in the presence of Zn^{2+} on all oligonucleotides tested with 5-BMF and on the RNA and DNA phosphorothioate oligomers with 6-IAF. Table 3B qualitatively depicts the fragmentation of the same oligonucleotides. In the presence of Zn^{2+} plus either alkylating agent, significantly more fragmentation occurred than in the absence of alkylating agent, likely because of alkylation forming phosphate triesters which are much more susceptible to hydrolysis than diesters.[56] Tb^{3+} in either alkylation solution was the most efficient fragmentation condition for RNA targets; in fact, Tb^{3+} plus alkylating agents even fragmented DNA.

Labeling with 5-BMF was slightly more effective than with 6-IAF for RNA oligomers in the presence of Zn^{2+} and Tb^{3+}, while in the absence of metal ions there was very little labeling by either alkylation agent. Oligonucleotide recoveries were generally high (≥90%, vide supra). A notable exception was found with all of the RNA oligomers in the presence of Tb^{3+} (65−75% recovery). These were the same oligonucleotides in which mass spectrometry detected many fragments, suggesting that Tb^{3+} catalyzed considerable fragmentation, resulting in poor recovery of small fragments (see ND samples in Table 3).

PAGE Analysis of Labeled Amplicons. Fragmentation, in addition to fluorescent labeling of amplicons, is necessary for efficient hybridization and accurate resequencing (i.e., >98% base calling, vide infra) of nucleic acid sequences on the Affymetrix GeneChip.[34] Preliminary experiments were undertaken to determine conditions that promote random but controlled fragmentation and alkylation of 313 nt RNA transcripts generated from *Mtb* 16S rRNA, transcripts that are equivalent to the amplicon products of transcription-mediated amplification (TMA;[57] a two enzyme isothermal amplification which alternately synthesizes cDNA and RNA transcripts, with RNA amplification efficiencies exceeding 10^9). This process was not as simple as it might initially appear; TMA solutions are complex mixtures of not only nucleic acids but also of various solutes and proteins, any of which can interfere with the labeling and/or fragmentation reactions. Phosphorothioates were not

(56) Westheimer, F. H. *Science* **1987**, *235*, 1173−1178.
(57) McDonough, S. H.; Bott, M. A.; Giachetti, C. In *Molecular and Laboratory Medicine Series; Nucleic Acid Amplification Technologies: Application to Disease Diagnosis*; Lee, H. H., Morse, S. A., Olsvik, Ø., Eds.; Eaton Publishing Company: Natick, MA, 1997; pp 113−123.

Table 4. PAGE Analysis of Concentration-Dependent (A) Fragmentation and (B) Alkylation Product Distributions of *Mtb* RNA Amplicons by Metal Ions and 5-BMF

A. Fragmentation

		313 nt transcript[b]			~26–106 nt fragments[b]		
[metal ion], mM	volume[a] based on	Mn^{2+}	Zn^{2+}	Ce^{3+}	Mn^{2+}	Zn^{2+}	Ce^{3+}
0.1	phosphor			26 100 ± 2700			818 ± 257
1	phosphor	25 900 ± 1730	24 100 ± 3250		3000 ± 662	2530 ± 1730	
2.6	phosphor			15 300 ± 2500			2690 ± 1350
5	phosphor			14 200 ± 7920			4380 ± 7600
5.5	phosphor		17 500 ± 4200			2960 ± 1840	
10	phosphor		6950 ± 7060			4670 ± 3610	
30.5	phosphor	3570 ± 1630			5350 ± 1830		
60	phosphor	3290 ± 2320			5860 ± 3470		

B. Alkylation

		~26–106 nt fragments[b]		
[5-BMF], mM	volume[a] based on	Mn^{2+}	Zn^{2+}	Ce^{3+}
0.01	fluorescence	10 100 ± 7000	6100 ± 3190	10 300 ± 6010
0.1	fluorescence	39 000 ± 6560	30 700 ± 17600	88 300 ± 6630
1	fluorescence	476 000 ± 210 000	415 000 ± 179 000	527 000 ± 227 000

[a] Volume from the phosphor analysis is the background-corrected area of the gel examined times the mean pixel intensity; volume from the fluorescence analysis has not been background-corrected. [b] Values are mean volumes ±SD ($n = 3-7$). As points of reference, the volumes were 28 000, 1090, and 4390 for the untreated 313 nt transcript, the untreated 26−106 nt fragments, and the fluorescent volume signal from the untreated 26−106 nt region, respectively.

incorporated into the amplicons because the model studies indicated phosphorothioates were not necessary for efficient labeling and fragmentation (Figure 5 and Table 3). Furthermore, incorporation of phosphorothioates would be sequence dependent and could be variable because of differing enzymatic efficiencies with nonnatural substrates.

The fragmentation and alkylation products from different conditions were separated by denaturing PAGE (see Supporting Information) and quantified by phosphor and fluorescence imaging, respectively (Table 4). Because of the complexity of these experiments relative to the model studies, only three reactive metal ions were tested, and emphasis was placed on the more metal ion-sensitive alkylating agent, 5-BMF. Consistent with the model studies, metal ion concentration was the single most influential factor in fragmentation of the RNA transcripts. On the basis of the decrease in the amount of the 313 nt transcript and the concomitant increase in the amount of the ~26−106 nt fragments (preferred size range for hybridization), RNA fragmentation was increased by increasing metal ion concentration. Ce^{3+} had the greatest effect on fragmentation at the lowest concentrations, followed by Zn^{2+} and Mn^{2+}. While Zn^{2+} and Mn^{2+} catalyzed fragmentation similarly in imidazole, MOPS, and Tris, Ce^{3+} catalyzed fragmentation only in imidazole and MOPS buffers, with little difference between imidazole and MOPS as fragmentation buffers (data not shown). Although Ce^{3+} was the most reactive metal ion examined, using high concentrations of Ce^{3+} proved problematic because of considerable post-LDC metal ion precipitation.

As seems reasonable, the most significant factor in enhancing labeling of RNA transcripts was the alkylation agent. The amount of fluorescently labeled fragmentation products in the ~26 −106 nt size range increased as the concentration of 5-BMF increased from 0.01 to 1 mM for each metal ion (Table 4B). The concentration of DMF (from the 5-BMF stock solution) had a small negative effect of labeling in the presence of Mn^{2+} (data not shown). In contrast to the model studies, metal ion species or concentrations did not have a significant influence on alkylation of RNA transcripts within the concentration ranges examined, except that in their absence, labeling was negligible (data not shown). While the model study experiments indicated that increased alkylation resulted in increased fragmentation, no correlation was seen between 5-BMF concentration and fragmentation of RNA amplicons in the 5-BMF concentration range examined. Conditions were found, such as with ~30 mM Mn^{2+} or 5−10 mM Zn^{2+} and 0.1−1 mM 5-BMF, in which there was a balance in the distribution of low molecular weight fragments ranging from ~26−106 nt and significant labeling.

GeneChip Analysis of Labeled Amplicons. Quantification of fragmentation and alkylation on polyacrylamide gels suggested reasonable starting conditions for species identification experiments on the Affymetrix *Mycobacterium* GeneChip. Conditions spanning three types of metal ions and four concentrations of 5-BMF in 30 mM imidazole were examined. After amplifying from 10^5 copies of *Mtb* 16S rRNA with TMA, RNA amplicons were added to LDC reagents and incubated at 60 °C for 30 min. The labeled and fragmented amplicons were diluted into hybridization buffer (without an intermediate purification step) and allowed to hybridize on the GeneChip. Interrogation of the fluorescence of each probe tile indicated that the best conditions using Ce^{3+} and Zn^{2+} (at 1 and 10 mM, respectively) fall substantially short of the 98% of the bases called (identified) correctly needed for accurate reconstruction of the interrogated *Mtb* sequence (Table 5); higher Ce^{3+} concentrations and lower concentrations of Zn^{2+} resulted in lower numbers of bases correctly identified (data not shown). When no metal ions were included, the percent correct fell to ca. 50%; on average, there was no difference among the different interrogation positions on the tiles. Correct calling of the nt sequence was obtained only when Mn^{2+} was used as the metal ion. There was not a strong dependence of alkylation on Mn^{2+} concentration between 15 and 45 mM (data not shown), but, for a given set of otherwise constant conditions (e.g., 30 mM buffer and 30 mM Mn^{2+}), the median fluorescence intensity increased with increasing 5-BMF concentration. Thus, with as little as 0.1 mM 5-BMF and 30 mM Mn^{2+}, the percent correct increased to ca. 94%, while at 0.6 and 1 mM 5-BMF, the percent

Table 5. GeneChip Analysis of Alkylation and Fragmentation of *Mtb* RNA Amplicons by 5-BMF and Metal Ions

	% correct	median intensity (rfu)
0.2 mM 5-BMF 30 mM imidazole pH 6.0 1 mM Ce^{3+}	76.2	1716
0.2 mM 5-BMF 30 mM imidazole pH 6.0 10 mM Zn^{2+}	88.6	1263
0.6 mM 5-BMF 30 mM imidazole pH 6.8	53.0	2221
0.1 mM 5-BMF 30 mM imidazole pH 6.8 30 mM Mn^{2+}	93.5	1059
0.6 mM 5-BMF 30 mM imidazole pH 6.8 30 mM Mn^{2+}	98.4	2515
1 mM 5-BMF 30 mM imidazole pH 6.8 30 mM Mn^{2+}	98.4	4270

Scheme 1. Possible Sites of Electrophilic Addition on Nucleic Acids (5′-AG Shown)

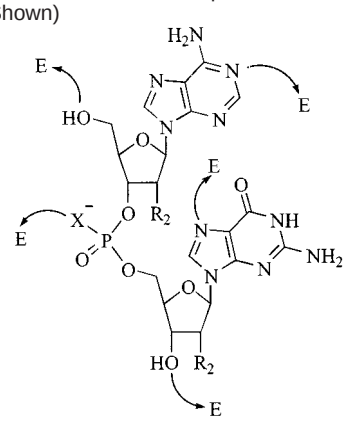

X = O; phosphate

X = S; phosphorothioate

R_2 = H; deoxyribose

R_2 = OH; ribose

E = electrophile

correct exceeded 98%. This high percentage corresponds to 182 of 185 interrogation positions, correctly identifying these samples as from *Mtb*. More generally, this shows that LDC can be used for processing nucleic acids for nucleic acid arrays from a complex milieu without the need for previous enzymatic labeling or postprocessing purification.

Discussion

The model studies, as well as the transcript product and microarray analyses, demonstrate that, beyond the obvious need for an alkylating agent to alkylate and metal ions to assist in degradation of nucleic acids, *alkylating agents are important for fragmentation, while metal ions catalyze alkylation*. Yet, what are the roles of the reagents in the reactions? To answer this within the confines of the current embodiment, it will be instructive to consider the results of the model studies.

Scheme 1 depicts several nucleophilic positions on nucleic acids that could react with electrophiles such as bromomethyl and iodoacetamido moieties. If alkylation occurs at the N1 of adenine or the N7 of guanine, considered the most nucleophilic base positions, fragmentation is not likely to proceed through a simple, random, phosphate scission mechanism but, rather, through patterned, base-alkylation, depurination degradations as in Maxam−Gilbert chemical sequencing reactions.[58] Likewise, fragmentation of the phosphodiester bonds is unlikely if alkylation takes place on the ribose alcohol groups. Nonetheless, both the base amines and the ribose hydroxyls could be sites of alkylation without concurrent fragmentation, consistent with stable mono- and dialkylation of nucleic acids (Figures 4A and 5A, Table 3).

The reactivities of the different electrophiles provide additional explanations for the chemistry of the reagents. Maleimide derivatives are thiol selective alkylating agents, yet allowing DNA containing internal or terminal thiophosphates (which, of course, are not thiols) to react with 5-MaF did not lead to appreciable labeling. Furthermore, addition of metal ions did not increase the product yield with 5-MaF. While alkyl halides and haloacetamides are also known to react with sulfur groups,[59,60] they are not as specific as maleimides for thiols;[61] on the other hand, bromomethyl and iodoacetamido functionalities have been shown to react with thiophosphates.[30−33,62−64] A terminal thiophosphate is less sterically hindered than an internal thiophosphate and, therefore, might be a more facile alkylation site. Indeed, DNA with a terminal thiophosphate labeled more efficiently with 5-BMF or 6-IAF than did phosphorothioate-containing DNA (Table 2). In addition, alkylation of a terminal thiophosphate results in a diester, which hydrolyzes slower than a triester formed by alkylation of a phosphorothioate.[56] No fluorescein labels on RNA fragments were detected by MS following treatment with 6-IAF and Tb^{3+} (Figure 5B). Also, the resulting phosphate groups were associated with the 3′-termini of the 5′-fragments. This explains the need for an alkylating agent for efficient fragmentation of RNA − formation of a phosphotriester intermediate from a phosphodiester or phosphorothioate linkage which breaks down to the 2′,3′-cyclic phosphate on the 5′-fragment, a 5′-hydroxy on the 3′-fragment, and a released mercapto-fluorescein derivative (Scheme 2), a pattern consistent with the mechanism of the ribozyme reaction.[65] The greater susceptibility of the phosphorothioate to fragmentation follows leaving group stability, $RS^- > RO^-$, and the differences in the pK_a values of thiols and hydroxyls. DNA fragmentation is presumed to follow a similar pathway, but, without the 2′-OH available to act with the high effective molarity of an intramolecular nucleophile, DNA must rely on the much lower molarity of H_2O, with a subsequent lower rate of fragmentation. The 3′-terminal phosphate may then become a favored site of stable alkylation, especially for DNA, with the formation of a new, stable diester.

(58) Maxam, A. M.; Gilbert, W. *Proc. Natl. Acad. Sci. U.S.A.* **1977**, *74*, 560−564.
(59) Alexiev, U.; Mollaaghababa, R.; Scherrer, P.; Khorana, H. G.; Heyn, M. P. *Proc. Natl. Acad. Sci. U.S.A.* **1995**, *92*, 372−376.
(60) Ansorge, W.; Rosenthal, A.; Sproat, B.; Schwager, C.; Stegemann, J.; Voss, H. *Nucleic Acids Res.* **1988**, *16*, 2203−2206.
(61) Griep, M. A.; Mesman, T. N. *Bioconjugate Chem.* **1995**, *6*, 673−682.
(62) Cosstick, R.; McLaughlin, L. W.; Eckstein, F. *Nucleic Acids Res.* **1984**, *12*, 1791−1810.
(63) Stewart, A. J.; Pichon, C.; Midoux, P.; Mayer, R.; Monsigny, M.; Roche, A. C. *New J. Chem.* **1997**, *21*, 87−98.
(64) Player, M. R.; Xiao, W.; Cramer, H.; Torrence, P. F. *Bioconjugate Chem.* **1998**, *9*, 137−142.
(65) Uhlenbeck, O. C. *Nature* **1987**, *328*, 596−600.

Scheme 2. Reaction Scheme for the Alkylation-Facilitated Fragmentation of RNA and Phosphorothioate-Substituted RNA

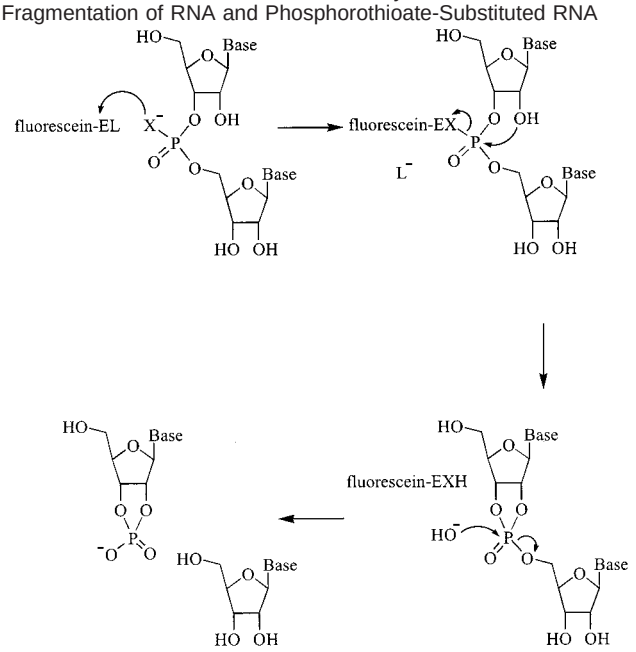

X = O; phosphate

X = S; phosphorothioate

E = electrophile

L⁻ = leaving group

Scheme 3. Model for Metal Ion-Assisted Alkylation of (Thio)phosphodiester Linkages

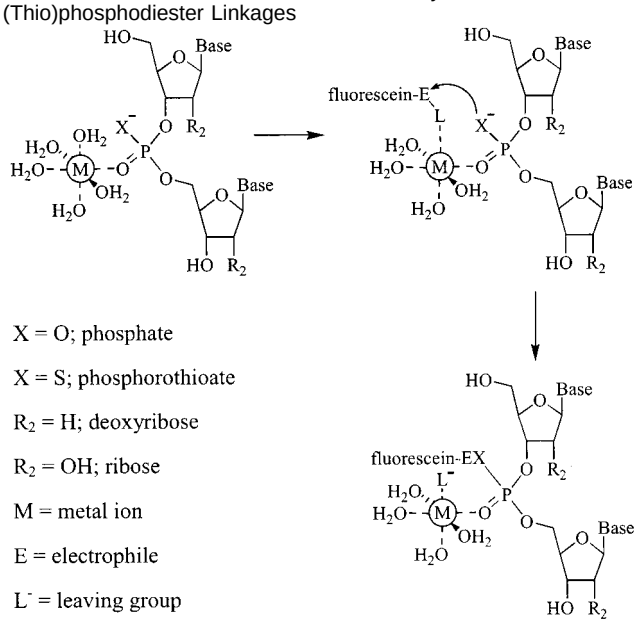

X = O; phosphate

X = S; phosphorothioate

R_2 = H; deoxyribose

R_2 = OH; ribose

M = metal ion

E = electrophile

L⁻ = leaving group

Interactions of metal ions with nucleic acids are well known.[66] To a first approximation in the present studies, trivalent metal ions tend to be more reactive in facilitating alkylation than are divalent metal ions, and these are much more reactive than monovalent metal ions (Figures 1 and 3, Tables 2−4). This could be because of differences in net charge, the fit of the metal ions into a nucleic acid structure, the affinity of metal ions for nucleic acids, or the reactivity of the metal ions. Fragmentation of mixed sequence RNA was found to be roughly random (Figure 5B), and because the different bases have different metal ion affinities and nucleophilicities, the metal ions and alkylating agents are not likely associating with or coupling to the bases as intermediates in the fragmentation process. Several structural studies indicate that most metal ions first populate a single phosphate oxyanion,[67−69] consistent with metal ion to phosphate affinities > metal ion to nucleobase affinities.[70] While correlations were not found between alkylation and metal ion to phosphate association constants, alkylation assistance of fragmentation is likely to occur at a nonbridging oxygen or sulfur of phosphate or phosphorothioate (as shown for electron-deficient pyrrolo[1,2-*a*]benzimidazoles),[71] and, hence, it seems reasonable that metal ion assistance is also in this vicinity.

Kuimelis and McLaughlin did not find a relationship between metal ionic radii and fragmentation rates of a ribozyme, nor did they find a correlation between the pK_a values of hydrated metal cations and fragmentation rates.[37,46] Their results suggest that there is little requirement of a particular metal ion radius within the range tested and that the metal ion cofactor does more than assist in deprotonating the 2′-hydroxyl group through a general base mechanism. No correlations were found between alkylation efficiencies and metal ion oxidation states, ionic radii, or metal ion-purine association constants in the current studies either (data not shown). Yet, Kuimelis and McLaughlin did observe a direct correlation between the "softness" of the metal ions (i.e., the hard−soft acid−base, or HSAB, principle)[72−74] and the rate of hydrolysis.[46] In the current studies, the most robust labeling conditions always included borderline-to-hard Lewis acids (e.g., Yb^{3+}, Ce^{3+}, Pb^{2+}, Zn^{2+}), implying that their reactivities are likely associated with hard Lewis bases such as oxygen rather than soft, sulfur-containing groups.

The lack of "symbiosis", or hard-with-hard and soft-with-soft acid−base character, found implies that the metal ions are not strongly involved with sulfur or oxygen nucleophiles in the alkylation step or with the fluorescent leaving group in the degradation step. Instead, the facile alkylation and degradation of the thiophosphate are because of the increased nucleophilicity and decreased pK_a (∝ stability of the leaving group) of the sulfur moiety relative to the oxo. Therefore, a simple explanation using the above evidence requires two distinct capacities for the metal ions. First, whether the nucleic acid is RNA or DNA, a metal ion coordinates with a nonbridging oxygen (Scheme 3).[67−69] This provides a proximal ligand site to assist the halide leaving group and increase the electrophilic nature of the bromomethyl or iodoacetamido moiety. The same is not true for maleimide, and, hence, metal ions do not increase the alkylating reactivity of 5-MaF in this case. Second, metal ions can catalyze degradation of both RNA *and* DNA. The metal ions are not interacting with the fluorescent leaving group, but, on the basis of 5′-phosphorothioate chemical fragmentation studies,[46] they

(66) Sigel, H. *Chem. Soc. Rev.* **1993**, 255−267.
(67) Alexander, R. S.; Kanyo, Z. F.; Chirlian, L. E.; Christianson, D. W. *J. Am. Chem. Soc.* **1990**, *112*, 933−937.
(68) Tajmir-Riahi, H. A.; Ahmad, R.; Naoui, M. *J. Biomol. Struct. Dyn.* **1993**, *10*, 865−877.
(69) Schneider, B.; Kabeláč, M. *J. Am. Chem. Soc.* **1998**, *120*, 161−165.
(70) Sigel, H.; Massoud, S. S.; Tribolet, R. *J. Am. Chem. Soc.* **1988**, *110*, 6857−6865.
(71) Schulz, W. G.; Nieman, R. A.; Skibo, E. B. *Proc. Natl. Acad. Sci. U.S.A.* **1995**, *92*, 11854−11858.
(72) Pearson, R. G. *J. Am. Chem. Soc.* **1963**, *85*, 3533−3539.
(73) Pearson, R. G. *Science* **1966**, *151*, 172−177.
(74) Parr, R. G.; Pearson, R. G. *J. Am. Chem. Soc.* **1983**, *105*, 7512−7516.

Scheme 4. Model for Metal Ion-Assisted Degradation of (Thio)phosphoester Linkages

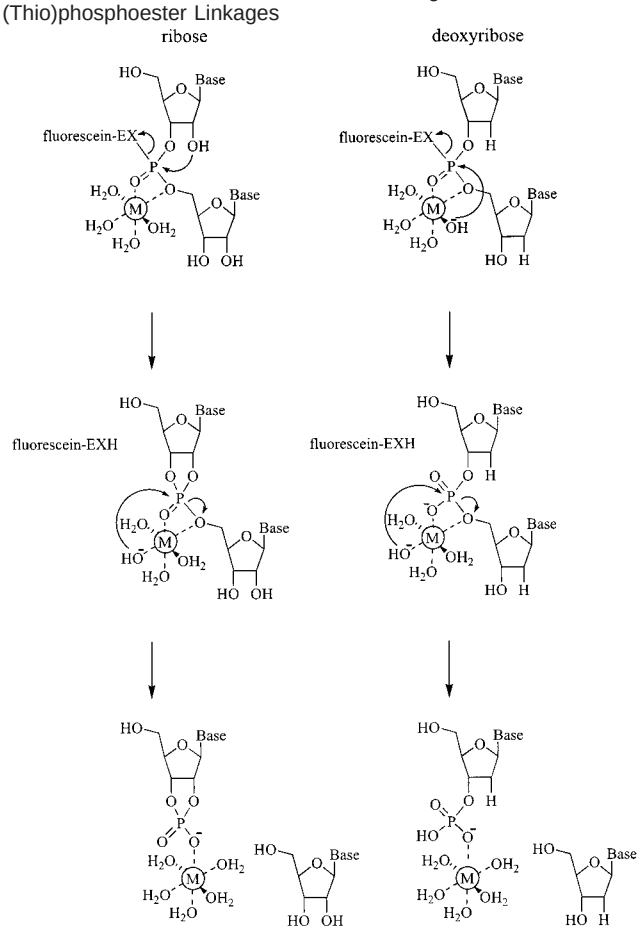

are likely interacting with at least the 5′-oxygen and possibly with the remaining nonbridging oxygen. In this manner, the metal ions are capable of increasing the electrophilicity of the phosphorus center, thereby catalyzing nucleophilic displacement of the conjugated fluorescein by the 2′-hydroxyl (RNA) or by a coordinated metal ion hydroxide on DNA (Scheme 4); both cases are intramolecular reactions. This coordination is not critical for the hydrolysis of the RNA-fluorescein triester, but it is for the decomposition of the RNA cyclic triphosphate and the DNA diester. Now the metal ion-ligated hydroxide nucleophilically displaces the 5′-nucleoside (as shown), while the metal ion stabilizes the incipient negative charge on the 5′ oxygen. Again, such descriptions are consistent regardless of the nucleophilic strengths of the nonbridging sulfur or oxygen moieties found in thiophosphates or phosphates or of the leaving group abilities of their triester products.

Thus, the described studies demonstrate a significant improvement for post-(bio)synthetic covalent coupling of fluorescent molecules onto nucleic acids; under appropriate conditions, the alkylation extent on nucleic acids can be increased by more than 100-fold with the addition of multivalent metal ions to bromomethyl- and iodoacetamido-activated fluorophores. The alkylations, in conjunction with metal ions, catalyze fragmentation of nucleic acids, including DNA. This is an additional advantage of the presented methodology because, as demonstrated, the described chemistries can be used to facilitate alkylation and fragmentation of amplicons in the same reaction mixture for analysis by hybridization, especially on microarrays. Labeling-during-cleavage chemistry is simple, fast, and occurs readily in aqueous solution with unmodified polynucleic acids; it is not limited to conjugating fluorophores, but other detectable labels (such as colorimetric, luminescent, or electron dense moieties) with alkyl halide and haloacetamide functional groups could be similarly attached to synthetic or natural nucleic acids or other appropriately derivatized biomolecules. There is some selectivity in that the reactivities of the metal ions differ depending on the alkylating agent and the form of the nucleic acid (RNA versus DNA, phosphate versus thiophosphate), following an explainable pattern, yet the selectivity is not too extreme to prevent efficient labeling of non-sulfur heteroatoms. Finally, under select conditions, alkylation/hydrolysis of RNA is uniform enough to allow convenient, rapid sequencing by mass spectrometry, even in the absence of phosphorothioate linkages needed in a previously described chemical sequencing method.[29]

Acknowledgment. This work was partly supported by bioMérieux Inc., Lyon, France. I am indebted to Chugai Biopharmaceuticals Inc. for use of their imaging equipment. For their technical assistance, I would like to thank M. Majlessi for oligonucleotide synthesis and HPLC separations, L. Tran for mass spectral work, and M. Jucker for generating some of the TMA products. Special thanks to M. Friedenberg, A. Laayoun, and A. Troesch for inspiring my interests in this undertaking.

Supporting Information Available: Tables and figures of fragmentation and alkylation products of amplified materials separated by PAGE and visualized by phosphor and fluorescence imaging, respectively (PDF). This material is available free of charge via the Internet at http://pubs.acs.org.

JA017746X